ANALYZING THE EFFECTS OF BLUE- GREEN-GREY INFRASTRUCTURE PATTERNS ON LAND SURFACE TEMPERATURE: A CASE STUDY OF HUE CITY

Do Thi Viet Huong[1], Nguyen Bac Giang[2], Nguyen Quang Viet[1], Doan Ngoc Nguyen Phong[1], Bui Thi Thu[1]
[1]Geography and Geology Faculty, Hue University of Sciences, 77 Nguyen Hue, Hue City, Vietnam
Email: dtvhuong@hueuni.edu.vn, nguyenviet.geo@gmail.com, phong080595@gmail.com, buithithu@hueuni.edu.vn
[2]Environmental Science Faculty, Hue University of Sciences, 77 Nguyen Hue, Hue City, Vietnam
Email: ngbgiang@hueuni.edu.vn

KEY WORDS: spatial landscape metrics; infrastructure patterns; LST; multiple regression, Hue City

ABSTRACT: City is considered as a main source of greenhouse gas emission which might cause environmental modification, such as urban heat island (UHT) phenomenon, ecosystem fragmentation and degradation. The role of Blue-Green-Grey infrastructure (BGGI) in mitigating the UHI effects has become a hybrid approach for sustainable urban under climate change. In this paper, the combination of remote sensing, GIS, and spatial landscape metrics was conducted to analyze the relationship between BGGI and land surface temperature (LST) of Hue City. The LST was extracted from Landsat 8 OLI/TIRS image, while BGGI was grouped from land use/land cover was classified from Sentinel-2A image. The spatial landscape metrics, including the percentage of landscape (PLAND), edge density (ED) were calculated for BGGI by using 10 x10 pixel grid. The multiple regression analysis between landscape metrics and LST show a high adjusted R2 value at 0.816 ($p<0.05$). In which, the PLAND of Blue and Green infrastructure contribute to decreasing LST (β = -0.725 and 0.780, respectively). Conversely, the ED of Grey infrastricture has a negative contribution on increasing the LST (β = 0.080). In addition, the ANOVA test result demonstrates the Blue and Green infrastructure help the LST ease by approximately 2^0C and 3.5^0C compared to Grey infrastructure ($p <0.05$). The findings from this study will contribute to providing a significant basis information for urban planning in orienting green space.

1. INTRODUCTION

Rapid urbanization and climate change are two challenges to sustainable urban development, so governmental authorities pay much concern about how to mitigate their unexpected impacts by urban planning. The process of urbanization has changed natural vegetation types to artificial cover layers, and subsequently increased impervious surface area. The artificial surfaces absorb and emit more solar radiation than natural areas so that it increases the urban thermal leading to so-called urban heat island effect (UHI) (Schwarz et al., 2012). Therefore, finding ways to reduce land surface temperature (LST) becomes a major concern in urban and eco-urban planning (Zhou, W. et al., 2017).

The role of Blue-Green-Grey Infrastructure (BGGI) in mitigating the impacts of the UHI has been introduced as an integrated approach to achieve urban sustainability under climate change. Urban green infrastructure is an important component in urban ecosystems, providing various ecosystem services. Strategies to ameliorate urban temperature through green infrastructure can be implemented by using vegetation cover with major forms of the greening of green roofs, planting trees and, increasing vegetation (N. Kabisch et al., 2017; Labib & Harris, 2018; Alves et al., 2019; Ahmed Sanjana et al., 2019).

Quantitative studies on the contribution of green infrastructure to heat reduction in urban areas have been mentioned by many studies (Bowler et al., 2010; Escobedo et al., 2019; Marando et al., 2019). The effective role of green infrastructure to heat reduction depends on the coverage, shape, size, and spatial scale of urban green spaces (Kong, F. et al. 2014; Li, X. et al., 2013). The larger the ratio of green space area, the better the cooling effect (Guo et al., 2019; Jaganmohan et al., 2016; Park et al., 2017). Landscape Metrics are often used to quantify the relationship between cover layer characteristics and their potential to reduce the LST (Buyantuyev A., 2010; Connors J.P., et al, 2013).

The impact of green space on heat mitigation can be measured using remote sensing at different spatial scales. Using satellite data to obtain detailed information on spatial distribution of land use/land cover in conjunction with the LST datasets have been carried out by numerous studies (Cao et al., 2010; Tran, Uchihama, Ochi and Yasuoka, 2006). The relationship between the LST and green space was examined by using regression analysis in some antecedent studies (Zhou et al., 2011; Guo et al., 2019).

In recent years, Hue City has been implementing new urban area projects to improve and create a living environment that accommodates the needs of all people in the city. In particular, the role of green space and natural landscape is indispensable in the process of urban development planning, especially the action plan of Hue green city in the orientation to 2030. Otherwise, Thua Thien Hue province in general and Hue City in particular are moving towards

a smart city whereby applying digital technology in researching environmental resources issues. Therefore, the integrated approach by remote sensing, GIS and spatial statistics to quantify the relationship between the LST and green space significantly contributes the scientific basis of the modern geographic space arrangement to establish further practical plans under the context of climate change. In general, previous studies highlighted the effect of plants or green space patterns on temperature, while quantitative investigation on the role of green infrastructure via its landscape metrics to the LST has not been paid much attention. Therefore, our main research objective aims to (1) measure the landscape indices of Blue-Green-Gray infrastructure (2) explore the effect of Blue-Green-Gray infrastructure pattern on the LST and (3) investigate the cooling effect of Blue-Green-Gray infrastructure pattern on the LST.

2. STUDY AREA AND MATERIALS

2.1 Study area

Hue City - the heritage city of Thua Thien Hue Province, is located in the center of Vietnam with an area of 71.69 km^2 and the urban population of 358,754 persons (2018) (Figure 1). The region is characterized by a tropical climate, two seasons with little rainy and rainy season. In which, the annual rainy season extends from August to January with an average temperature of 20-22^{0}C. While the less rainy season is from February to July, with an average temperature of 27-29^{0}C and the highest temperature reaches to 38-40^{0}C in May and June. Hue City is well-known as a green city, and was honored as an "ASEAN Cultural City" and "ASEAN environmental sustainability City" in 2004. However, Hue City has been experiencing a rapid urbanization that makes green and blue infrastructure gradually decrease due to the expansion of impervious surface (grey infrastructure), and unequally distribute across the city. Therefore, green space reduction in combination with risk of climate change and natural disasters are now great challenges that require the local government to tackle to assure the sustainable goals in the future.

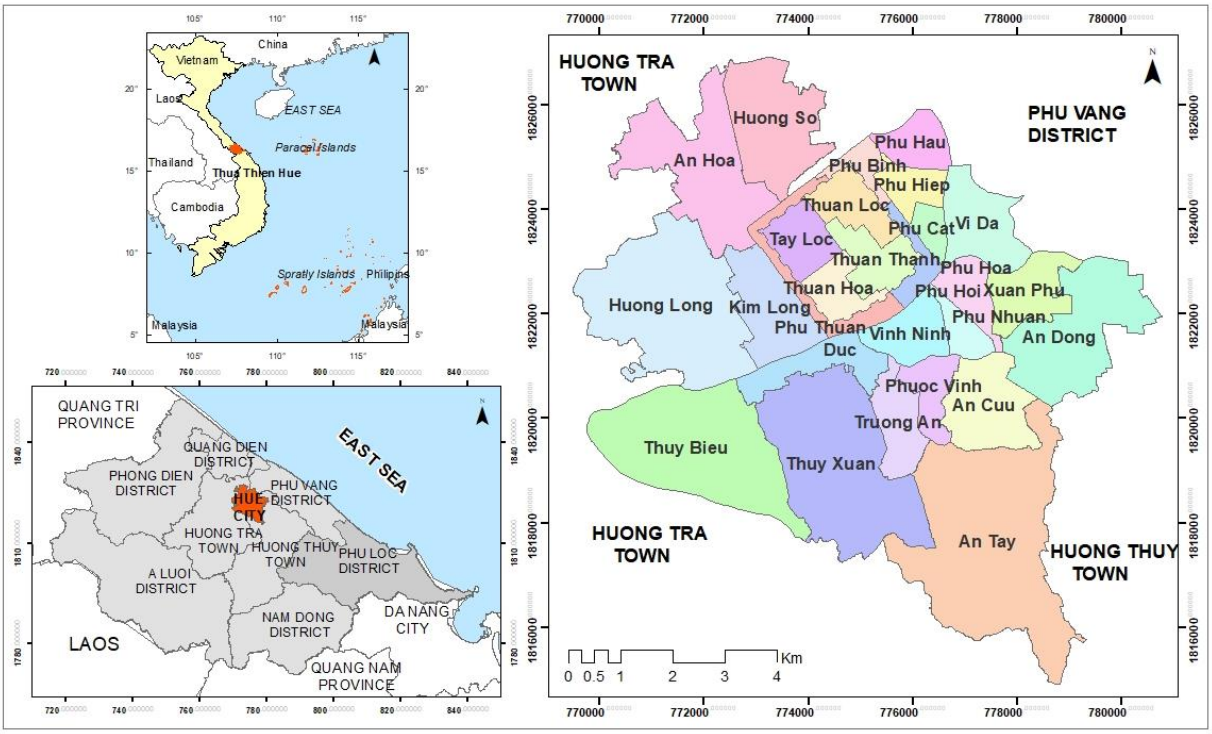

Figure 1. The location of Hue city

2.2 Data acquistion

In this study, Landsat 8 Operational Land Imager (OLI) and Thermal Infrared Sensor (TIRS) were collected on April 25, 2019, download free from Earth Explorer (http://earthexplorer.usgs.gov) were utilized to derive the LST. Sentinel -2 image at Level-2A, acquired on April 11, 2019, including band 2, 3, 4, 5, 6, 8 A, 11, and 12 with resolution 20 x 20 m download free from Land Viewer - EOS (https://eos.com/landviewer/) used to extract the LULC and Blue-green-grey infrastructure. The Level-2A product provides Bottom of Atmosphere (BOA) reflectance images derived from the associated Level-1C products, and each Level-2A product is composed of 100 x 100 km^2 tiles in cartographic geometry (UTM/WGS84 projection) (Suhet, 2015). Both Sentinel -2A and L8 images contain less than 8% cloud

coverage, mainly located at the corner of the scene, and 0% cloud coverage over the study area is suitable for processing. The existing GIS base data of Hue city also is collected as administrative maps for this analysis. The spatial data image was projected into the VN-2000 coordinate system using GIS base data.

3. METHODOLOGIES

3.1 Land use/land cover and Blue-Green-Gray infrastructure classification

All the bands 2-7, 8A and 11-12 in 20 m resolution of Sentinel 2A image was experienced a pre-processing on ArcGIS Desktop Software for further classification. Object-based image analysis has been applied more frequently for Sentinal-2A satellite image classification than pixel-based analysis in urban green space, green infrastructure mapping and monitoring. Object-based approach reveals various advantages, which enables users to combine spectral information and spatial information for extracting target objects, improving image class, and integrating ancillary data in the process (Gaurav K. P. & Prasun K. G., 2010; Tamta et al. 2015; Labib & Harris, 2018; Benchelha et al., 2019).

Therefore, the object-based classification was selected in this study to interpret LULC types. The eCognition software 9.1 were used via the class hierarchy to define the threshold of the calculated Normalized Difference Build-up Index (NDBI) and default indices. The formulation for calculating NDBI indices was presented as follows:

$$NDBI = (SWIR - NIR)/(SWIR + NIR) \quad (1)$$

In case of Sentinel-2A imagery, the SWIR is the reflectance corresponding to the shortwave- infrared spectral band (band 11) and NIR is the spectral reflectance of the near-infrared band (band 8). The Normalize Difference Build-up Index value lies between -1 to +1. Negative value of NDBI represents water bodies, whereas higher value indicates build-up areas. NDBI value for vegetation is low (Zha et al., 2003).

Six LULC categories were identified from image classification, namely built-up land, water body, agricultural land, forest land, trees, shrubs & grass land, and bare land. Green-Blue-Grey infrastructure (GBGI), Blue-Green Infrastructure (BGI), or green infrastructure, blue infrastructure are the trend terms used in landscape planning, land use planning, ecosystem service response to flood risk and climate change adaptation in the context of urban development strategy (N. Kabisch et al., 2017; Labib & Harris, 2018; Alves et al., 2019; Ahmed Sanjana et al., 2019). Therefore, the BGGI was classified by following the LULC categories in this study as listed in table 1.

The accuracy of LULC classification was assessed using 180 "ground truth" points data collected from the fieldwork on June 2019. Some accuracy measures derived from the error matrix were used, including the overall accuracy and the Kappa coefficient. The Kappa value (k) is from 0 to 1, in which $k \geq 0.8$ represents strong agreement and good accuracy, $0.4 \leq k \leq 0.8$ is moderate accuracy and $k \leq 0.4$ is poor accuracy (R. G. Congalton, 1991).

Table 1. Identifying the Blue-Green-Grey infrastructure perspective to LULC types

Blue-Green-Grey Infrastructure	Elements	LULC categories group proposed
Blue Infrastructure (BI)	Natural features: rivers, ponds, lakes, canal, wetlands	Water body (Wa)
Green Infrastructure (GreenI)	Natural vegetation: urban parks, trees, private and public open spaces, forest, agriculture, grass	Agricultural land (AgL), Forest land (FoL),Trees, shrubs & grass land (TSGrL)
Grey Infrastructure (GreyI)	Manmade elements: built-up, engineered and physical structure, concrete materials, roads, barren land and other urban constructions...	Built-up land (BuL), bare land (BaL)

3.2 Land surface temperature extraction from Landsat image

The LST represents the heat energy emitted from the buildings, land and the other surfaces of the earth, and LST is one of the key parameters in surface energy balance and regional climates (Xiangchen Meng et al., 2018; Aliihsan Sekertekin & Stefania Bonafoni, 2020).

Firstly, the digital number (DN) of the thermal band from the Landsat 8 TIRS (band 10: 10.6 - 11.19 µm) with 100 x 100 m resolution) were converted to top-of-Atmospheric (TOA) spectral radiance:

$$L\lambda = ML\ Qcal + AL \quad (2)$$

where L_λ is the TOA spectral radiance (Watts/(m² *sr*µm), $Qcal$ is the pixel value (DN), and ML and AL are rescaling coefficients (United States Geological Survey (USGS), 2019).

Secondly, TOA spectral radiance was transformed to TOA brightness temperature using thermal conversion constants

provided in the metadata of Landsat 8 OLI/TIRS image in degrees Celsius (^{0}C):

$$T_b = \frac{k_2}{Ln(\frac{k_1}{k_2}+1)} - 273.15 \quad (3)$$

where T_b is the TOA brightness temperature in Celsius; K_1 is the thermal conversion constant for the band 10 (K_1_CONSTANT_BAND_n from the metadata), K_2 Thermal conversion constant for the band 10 (K_2_CONSTANT_BAND_n from the metadata).

Finally, the LST in Degrees Celsius (°C) was estimated from the calculated using Planck formulation:

$$LST = \frac{\text{Tb}}{1+(\frac{\lambda * \text{Tb}}{\text{a}}) * ln\varepsilon}, \quad (4)$$

where λ is the center wavelength for band 10 (10.9 µm); $\rho = h * c/\sigma$, where h is the Planck constant (6.626 x 10^{-34} $J * s$), c is the velocity of light (2.998 x 108 m/s), σ is the Boltzmann constant (1.38 x 10^{-23} J/K); ε is the land surface emissivity.

The Normalized Difference Vegetation Index (NDVI) was utilized to estimate land surface emissivity ε by equation suggested by Yuan F, Bauer M. (2007).

$$NDVI = \frac{\text{NIR} - \text{R}}{\text{NIR} + \text{R}}, \quad (5)$$

where NIR is the spectral reflectance corresponding to the near-infrared band of OLI-TIRS (band 5) and R the spectral reflectance of the red band of the band 4.

The land surface emissivity ε was derived using an equation given by Sobrino, J.A. et al. (2008).

$$\varepsilon = \text{mPv} + \text{n}, \quad (6)$$

where Pv is the vegetation coverage, the constant values for the emissivities of vegetation and bare soil, m and n were calculated as 0.004 and 0.986, respectively.

Using the NDVI data, the vegetation coverage Pv was estimated using the following equation:

$$P_v = (\frac{\text{NDVI} - \text{NDVI}_{\text{min}}}{\text{NDVI}_{\text{max}} - \text{NDVI}_{\text{min}}})2, \quad (7)$$

where NDVImax and NDVImin are the maximum and minimum vegetation index in the study area, respectively.

3.3 Landscape pattern metrics analysis

Landscape is defined as a heterogeneous land area composed of a cluster of interacting ecosystems that is repeated in similar form throughout (McGarigal K., Marks B.J., 1995) and is composed of a hierarchy of patches mosaic across the range of scale.

In our work, two landscape metrics were selected to examine the effect of BGGI on the LST (table 2) that included percentage of landscape (PLAND) and edge density (ED). The PLAND refers to the proportion of all patches of a certain patch type in the total landscape area. Its function is to quantify the proportional abundance of a certain patch type in the landscape. The ED represents the sum of the lengths of all edge segments involving the corresponding patch type, divided by the total landscape area.

The landscape metrics according to McGarigal and Marks (1995) were calculated following the landscape structure analysis program FRAGSTATS version 4.2.
(http://www.umass.edu/landeco/research/fragstats/documents/fragstats_documents.html). It requires a user specifies the level of heterogeneity at class or landscape, and the shape (round, square or hexagon) and window size to be used for landscape metric statistic. In this study, a 10x10-pixel window was designed to calculate two landscape metrics.

Table 2. Landscape metrics for analyzing blue-green-grey infrastructure patterns

Metrics (abbreviation)	Unit	Formulation	Description
Percentage of landscape (PLAND)	%	PLAND = 100/A x $\sum_{i=j}^{n} a_{ij}$ (8)	PLAND = proportion of the landscape occupied by patch type (blue, green, gray) i a_{ij} = area (m^2) of patch (blue, green, gray) ij A = total landscape area (m^2)
Edge Density (ED)	m/ha	ED = 10,000/A x $\sum_{k=1}^{m} e_{ik}$ (9)	e_{ik} = total length (m) of edge in landscape involving patch type (blue, green, gray) i A = total landscape area (m^2)

3.4 Statistical analysis

The plotted value of mean LST per each element of blue, green and grey infrastructure pixel were extracted for analyzing the LST variation and its relationship with BGGI. Analysis of variance (ANOVA) with Welch test was employed to examine the significant difference among BI, GreenI and GreyI in controlling the LST.

The post hoc test was also conducted for clarifying how different in the LST between the groups of BGGI elements. A p-value (< 0.05) was considered a significant means (Field 2013). In addition, we used the multiple-linear regression as a statistical model to examine the linkage between the LST and BGGI landscape pattern metrics through R^2, p-value, standard coefficients β, as well as variance inflation factor (VIF). The mean value of the LST and spatial landscape metrics of BGGI elements in grid cell 10x10-pixel window created by fishnet tool were used for statistics. All statistical implementations were performed using the IBM SPSS version 26.

4. RESULTSS

4.1. Blue-Green-Gray infrastructure distribution

4.1.1. Land use/Land cover classification

The hierarchical scheme object-based classification of five levels in each image was implemented by approaching fuzzy membership functions (Figure 2). The classified features were extracted following the defined rule set classification, in which mainly threshold of default indices (NIR, Green, Brightness, Max.diff) and Normalized Difference Built-up Index (NDBI), were utilized for achieving LULC classes (Table 3).

Table 3. Segmentation level of classified features from Sentinel 2 - Level 2A

Segmentation level	Parameter (Scale, shape, compactness)	Number of fragmentation	Classified features	Parameter threshold
Level-1	30, 0.3, 0.7	6,729	Water body	NIR ≤ 1,820
			Land	NIR > 1,820
Level-2	15, 0.3, 0.7	29,664	Vegetation	NDBI <-0.1
			No vegetation	NDBI ≥ -0.1
Level-3	15, 0.3, 0.7	29,674	Bare land	Brightness>2,500
			Built-up land	Brightness≤2,500
Level-4	50, 0.3, 0.7	20,637	Forest land	Green<530
			Other vegetation land	Green≥530
Level-5	15, 0.1, 0.5	32,281	Agricultural land	Max.diff≥1.8
			Trees, shrub & grass	Max.diff<1.8

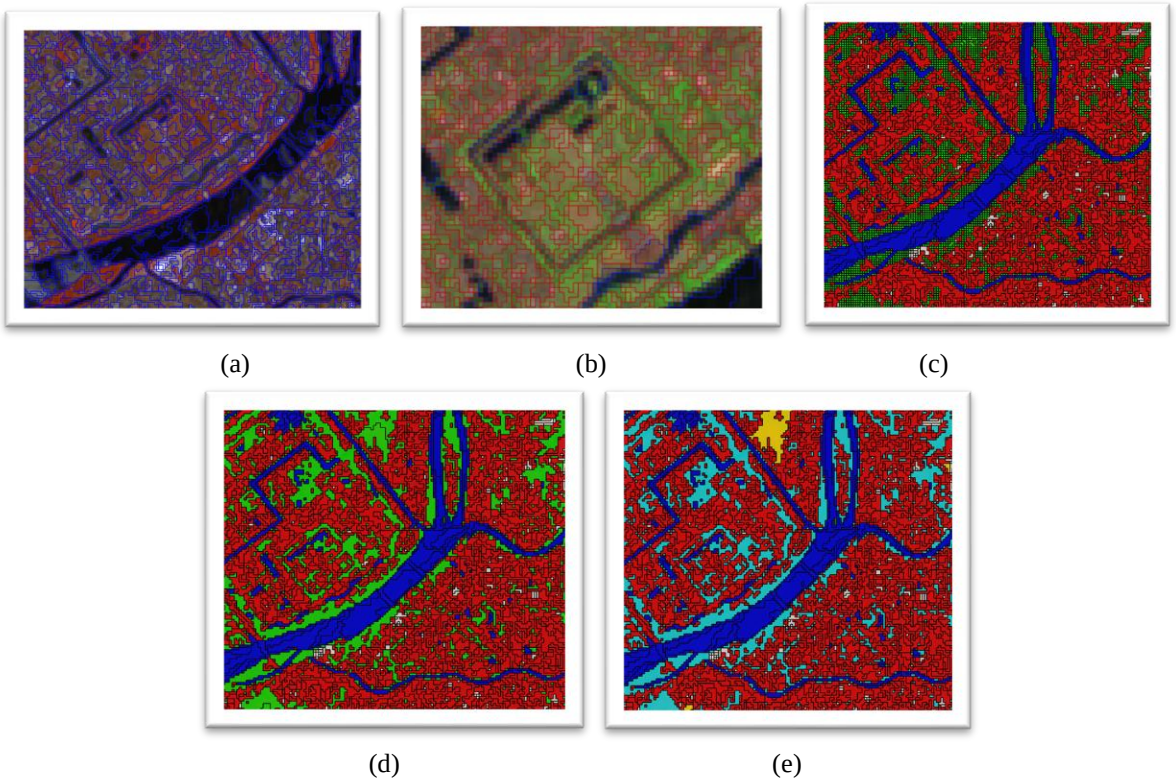

Figure 2. Level of fragmentation of Sentinel 2- level 2A (a) Level-1, (b) Level-2, (c) Level-3, (d) Level -4, and (e) Level-5

The final LULC map was represented in figure 3. The accuracy of classification performance was validated by using quantitative measures, including overall accuracy and kappa coefficient (Table 4) for the six LULC types. The overall accuracy of LULC map was 81% and the kappa index value was 0.83. These values were acceptable and agreeable for analyzing the landscape pattern.

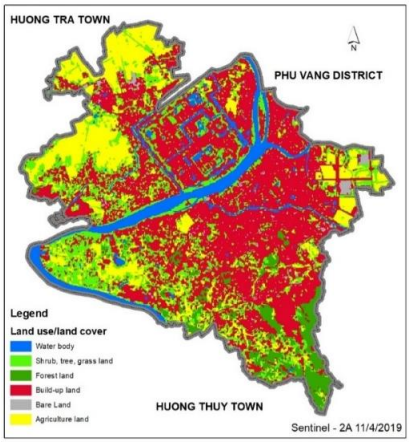

Figure 3. LULC map for 2019 of Hue City

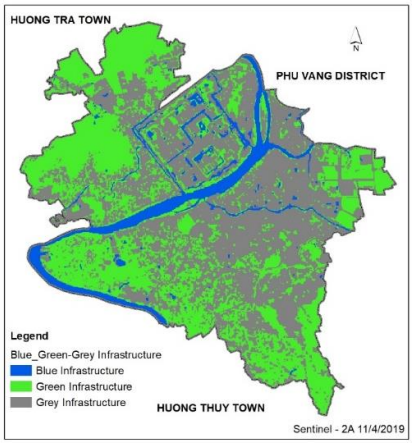

Figure 4. Distribution of Blue-Green-Grey infrastructure

Table 4. Accuracy matrix of classified LULC map

Classified Sentinel 2A image data	Ground truth data						Total
	AgL	BaL	BuL	TSGrL	FoL	Wa	
AgL	25	0	3	1	0	0	30
BaL	0	18	12	0	0	0	30
BuL	0	0	27	3	0	0	30
TSGrL	0	0	5	25	0	0	30
FoL	0	7	0	0	23	0	30
Wa	0	0	0	2	0	28	30
Total	25	25	48	31	23	28	180
Overall accuracy				81%			
Kappa Coeffcient				0.83			

4.1.2. Blue-Grey-Green infrastructure mapping

The map of BGGI was produced by regrouping the resultant LULC types as followed the defined of BGGI elements (Table 2). The figure 4 and table 5 showed the area and proportion of each BGGI element of the study area in the year 2019.

Table 5. Area and occupancy of Blue-Green-Grey infrastructure in 2019

Element of BGGI	**LULC categories**	**Area (ha)**	**Occupancy (%)**
Blue Infrastructure	Water body	605.28	8.45
Green Infrastructure	Trees, Shrubs & Grass; Forest land; Agricultural land	309.08	43.27
Grey Infrastructure	Built-up land Bare land	3,456.20	48.27

The BI accounted a minor percentage of 8.45% including Huong river system, ponds mostly concentrated in the northern Huong River wards (Phu Hoa, Phu Thuan, Kim Long. The GreyI apparently occupies the highest proportion at 48.27%, mainly distributed in the center and south wards such as Citadel areas, Vinh Ninh, Phu Hoi, Xuan Phu, Phuoc Vinh, Vi Da… The GreenI accounts for 43.27%, concentrated in the fringe of city and high density in Huong So, Huong Long, An Tay and Thuy Bieu ward where the agriculture and forest land were observed. Besides, a mixture pattern of the GreenI, BI and GreyI was seen in the Citadel area and Kim Long ward.

4.2 Spatial distribution of landscape metrics indices

The spatial pattern of the PLAND and ED for the BGGI was illustrated at figure 5 and 6. The PLAND indices showed a different magnitude in spatial distribution for GreenI, BI and GreyI density. Higher PLAND_BI was seen along

Huong River and lakes in Hue Citadel, which its value ranged from 40 to 100%. The remainder areas mainly obtained a lower value under 20%. As for the PLAND_GreenI, the areas far away from central urban had a higher value than others. The PLAND index of over 60% covered a large areas located in the western site of Hue City where is mostly planted by agricultural crop, forest, etc. However, built-up land which was dominated in the eastern site leads to decrease the PLAND_GreenI value close to under 20%. Conversely, the PLAND_GreyI illustrates an opposite pattern to PLAND_GreenI, in which the areas along Huong River and the eastern site of Hue City had a higher value than other areas with a range from 60 to 100%. The dominated built-up land that concentrates in the center city might amplify the UHI effects.

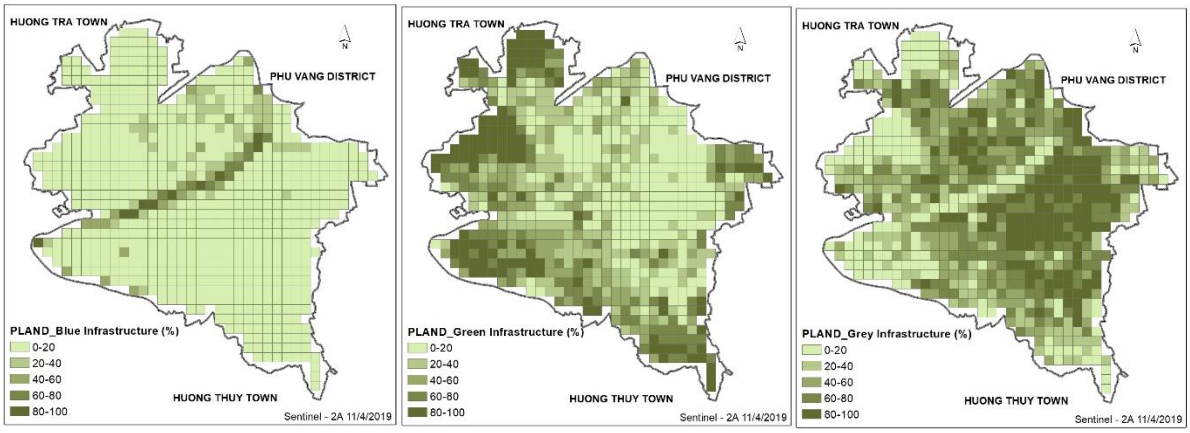

Figure 5. PLAND indices of Blue, Green and Gray Infrastructure

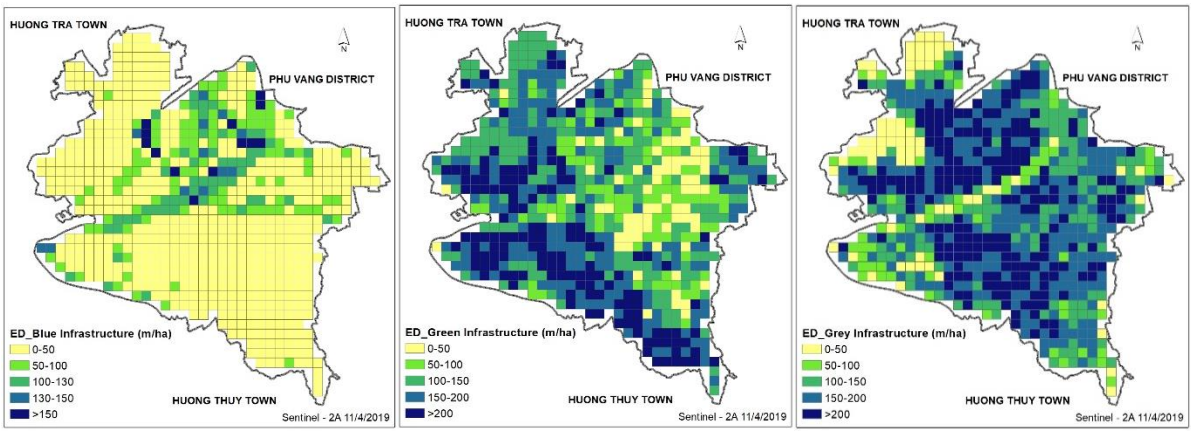

Figure 6. ED indices of Blue, Green and Gray Infrastructure

As seen in figure 6, a higher value of ED value for BI was observed at areas along and surrounding water body (river and lake), while a large area in the north and south had a lower value at under 50 m/ha. The ED value of GreenI tended to decrease from all sites to the center city, however it also shows that the Green Infrastructure at western site was slightly fragmented more than other sites. As for the ED_GreyI, its value was significantly high at all areas within Hue City, except for partially northern site.

4.3 Urban land surface temperature retrieval from Landsat 8

The LST retrieved from Landsat image of Hue City was showed in figure 7. The LST in 25th of April, 2019 was found at a wide range from 26.27 to 36.16^{0}C. The highest temperature was evidently observed in center of Hue City like Phuoc Vinh, Truong An, An Cuu, Phu Hoi, Xuan Phu (south and south east of city). In contrast, the areas far from the central city where vegetation coverage areas were

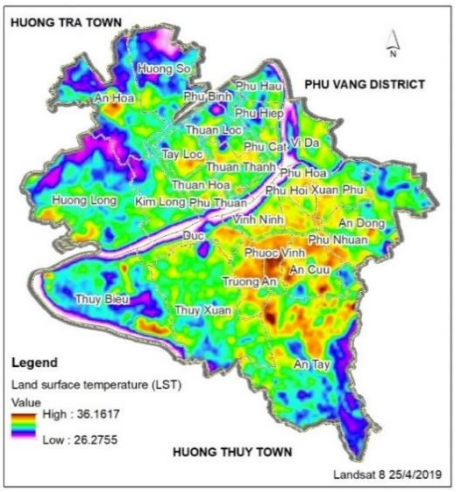

Figure 7. Land surface temperature calculated for Hue city

dominated by forest land (An Tay ward) and agricultural land (An Hoa, Huong So, Thuy Bieu, An Dong) achieved a high rate of GreenI. As a result, this element might enable to reduce radiance absorption, and increase water evaporation.

Consequently, the LST in these areas was observed at a lower intensity than in the central area of the city. While the lowest temperature was suitable to spatial distribution of pond and moat system of Citadel region, Huong river corresponding to the BI element.

4.4 Effects of Blue-Green-Grey infrastructure pattern on the LST

4.4.1 LST differences among Blue-Green-Grey infrastructure

The LST value per BBGI pixel was extracted for analyze the different among the BGGI pattern. The boxplots of the LST for each BGGI were presented in figure 8 and 9. The significant different in the average LST of BGGI elements were observed. The figure 8 shows a higher mean LST in GreyI than green and blue infrastructure. The GreyI caused the highest average temperature mainly associated with the capacity of the construction of material, impermeable surface absorb more incoming solar radiation on the surface and delay release of heat with the lower limit of temperature is about 29.3^{0}C and the maximum temperature is 34.4^{0}C. GreenI had an average temperature approximately 30^{0}C and ranged from 27.5 to 32.5^{0}C, it is might be attributed to the variability of the agricultural and forest land of the city. The BI of the city occupies a small proportion in the central of the city whereby it has the important role in reducing the LST. From the boxplot, the temperature of BI shows a minimum value at about 26.27^{0}C, while its maximum value is about 36^{0}C. This figure is higher than that in GreyI. The mixed pixels between water bodies (ponds and moats system, channel, river) and bare land might to present the high LST values in BI because the spatial resolution of Landsat 8 OLI at 100x100m leads to bias the temperature surface.

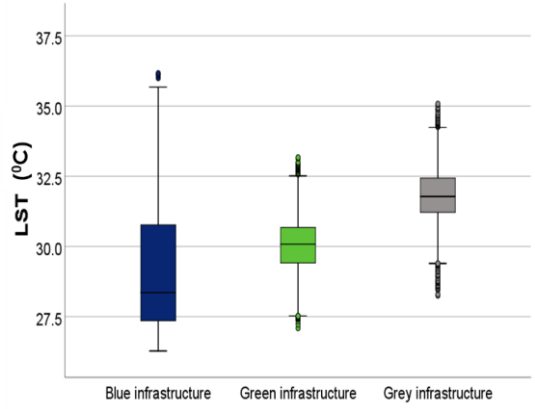

Figure 8. Boxplot of land surface temperature for BGGI

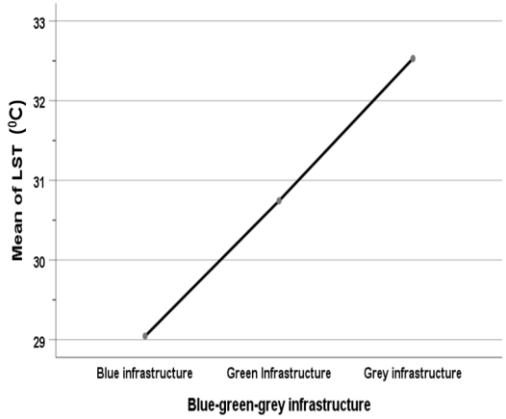

Figure 9. Mean plots of LST for BGGI

The result ANOVA test in the observed significance value of Levene statistic is less than 0.05, indicating the variance were unequal and the variances are significantly different (Table 6). Then the robust test of quality of means is examined with a value of Welch is significant (<0.05), referred the means of the groups are significantly different. Finally, the post hoc multi comparison was conducted with parameter of Games-Howell for discovering how different of the LTS of BGGI elements. In table 6, the mean LST is relatively different among BGGI, in which GreyI makes LST reach to 32.48^{0}C. The mean LST in BI is the lowest at 29^{0}C. Results indicates that BI and GreenI can decrease LST by approximately 2^{0}C and 3.5^{0}C in comparison with GreyI.

Table 6. ANOVA statistical analysis in the differences among Blue-Green-Grey infrastructure

ANOVA test (Post hoc tests: Tamhane)

Dependent Variable: LST

Independent Variable (I) BGGI		Mean Difference (I-J)*	Std. Error	Sig.	95% Confidence Interval	
					Lower Bound	Upper Bound
BI	GreenI	-1.698	0.025	0.000	-1.758	-1.638
	GreyI	-3.484	0.025	0.000	-3.544	-3.425
GreenI	BI	1.698	0.025	0.000	1.638	1.758
	GreyI	-1.787	0.008	0.000	-1.806	-1.768
GreyI	BI	3.484	0.025	0.000	3.425	3.544
	GreenI	1.787	0.008	0.000	1.768	1.806

*. The mean difference is significant at the 0.05 level.

4.3.2 Blue-Green-Grey infrastructure landscape pattern metrics and LST

The two landscape metrics of PLAND and ED were employed to analyze the effect of BGGI elements on the LST of Hue City. The result of multiple regression through enter method explained how effect of BGGI elements on the LST change, in which the LST is the dependent variable and 6 variables as PLAND_BI, PLAND_GreenI, PLAND_GreyI, ED_BI, ED_GreenI, ED_GreyI are the independent variables (Table 7). The regression model results in significant good degree of prediction with a high Pearson correlation R =0.904, adjusted value R2=0.816, and the .sig value less than 0.05. The PLAND_GreyI, ED_BI, ED_GreenI metric were removed from the model. The ED_GreyI, PLAND_BI, PLAND_GreenI metrics were determined with the best predictive performance with a significant value (.sig <0.05), in which the PLAND of Blue and Green Infrastructure contribute to decreasing LST (β = -0.725 and 0.780, respectively). Conversely, the ED of GreyI has a negative contribution on increasing the LST (β = 0.080).

Table 7. Multiple linear regression of landscape pattern metrics and LST

Variable		Standardized Coefficients βeta	Statistics			
			R	Adjusted R^2	Sig.	VIF
Dependent	Independent					
LST	ED_GreyI	0.080	0.904	0.816	0.00	1.657
	PLAND_GreenI	-0.730			0.00	1.735
	PLAND_BI	-0.695			0.00	1.314

From the regression formulation: LST = 0.080 * ED_GreyI - 0.730 * PLAND_GreenI - 0.695 * PLAND_BI, it can be interpreted that the PLAND_GreenI has more significant effect in mitigating the LST than PLAND_BI in the study area. Hence, increasing vegetation cover is the priority solution in urban planning under the context of climate change. In this study, with the assistance of GIS and RS techniques, we conduct successfully landscape pattern analysis for BGGI at 10x10 pixel grid and LST estimation. However, due to the lack of available ground-truth LST observation data, the LST retrieval from Landsat image is still uncertainty without validation performance. In addition, the size of grid in defining landscape pattern statistic might effect on the relationship not only between the LST and the ED of BGGI but also between the LST and the PLAND of BGGI. Therefore, it is necessary to attempt to do this investigation at smaller grid sizes and more landscape metric indices. From those, we can explore much more meaningful information on their relationship. Moreover, this study only highlights how green space impacts on the LST to provide general picture on its relation to the LST for urban planning purposes. For more detail, it is necessary to concern about connectivity, cost-distance analysis, etc. on purpose to design urban green spaces in the environmental protection and recreational areas.

5. CONCLUSION

This study applied GIS and RS techniques to obtain the spatial distribution of BGGI and the LST from Sentinel-2A and Landsat 8 OLI/TIRS images. To calculate the landscape metrics indices, 10x10 pixel grid was designed to compute the PLAND and ED, then statistical evaluation was performed to examine the relationship between BGGI and the LST. The multiple regression analysis between BGGU landscape metrics pattern and LST show a high adjusted R2 value at 0.816 (p<0.05). In which, the PLAND of Blue and Green Infrastructure contribute to decreasing LST (β = -0.725 and 0.780, respectively). Conversely, the ED of GreyI has a negative contribution on increasing the LST (β = 0.080). In addition, the ANOVA statistical analysis demonstrates that the BI and GreenI could help the LST ease by approximately 2^0C and 3.5^0C compared to GreyI. The findings indicate that more green spaces should be developed as a effectively potential solution reduce air temperature and increase relative humidity in urban areas. As a results, the ED metric will be an effective measurement for depicting the relationship between BGGI and the LST. The findings from this study will provide some significant basic information for urban planning in orienting green space.

References

Ahmed Sanjana, Mahbubur Meenar, & Ashraful Alam, 2019. Designing a Blue-Green Infrastructure (BGI) Network: Toward Water-Sensitive Urban Growth Planning in Dhaka, Bangladesh. Land, 8 (138), 1–21.R.

Aliihsan Sekertekin, & Stefania Bonafoni, 2020. Land Surface Temperature Retrieval from Landsat 5, 7, and 8 over Rural Areas: Assessment of Different Retrieval Algorithms and Emissivity Models and Toolbox Implementation. Remote Sensing, 12(294), 1–32. https://doi.org/doi:10.3390/rs12020294.

Alves, A., Gersonius, B., Kapelan, Z., Vojinovic, Z., & Sanchez, A., 2019. Assessing the Co-Benefits of green-blue-grey infrastructure for sustainable urban flood risk management. Journal of Environmental Management, 239, 244–254. https://doi.org/10.1016/j.jenvman.2019.03.036.

Benchelha, M., Benzha, F., & Rhinane, H., 2019. Object based "dayas" classification using Sentinel a-2 satellite imagery case study city of Benslimane. ISPRS - International Archives of the Photogrammetry, Remote Sensing and Spatial Information Sciences, XLII-4/W12, 33–39. https://doi.org/10.5194/isprs-archives-XLII-4-W12-33-2019.

Buyantuyev A., Wuj, 2010. Urban heat islands and landscape heterogeneity: Linking spatiotemporal variations in surface temperatures to land-cover and socioeconomic patterns. Landscape Ecology, 25(1), 17, 2010.

Cao, X., Onishi, A., Chen, J., Imura, H.,2010. Quantifying the cool island intensity of urban parks using ASTER and IKONOS data, Landscape Urban Plan, 96, 224–231.

Congalton G.,1991. A review of assessing the accuracy of classifications of remotely sensed data. Remote Sensing Environment, 37(1), 35–46 (1991), http://dx.doi.org/10.1016/0034-4257 (91)90048-B.

Connors J.P., Galletti C.S., Choww.T.L.,2013. Landscape configuration and urban heat island effects: Assessing the relationship between landscape characteristics and land surface temperature in Phoenix, Arizona. Landscape Ecology, 28(2), 271.

Guo G., Wu Z., Chen Y.,2019. Complex mechanisms linking land surface temperature to greenspace spatial patterns: evidence from four southeastern Chinese cities. Sci Total Environ 674: 77–87.

Jaganmohan M, Knapp S, Buchmann CM, Schwarz N.,2016. The bigger, the better? The influence of urban green space Landscape Ecol design on cooling effects for residential areas. J Environ Qual, 45(1):134–145.

Kabisch N. et al.,2017. Nature-based Solutions to Climate Change Adaptation in Urban Areas, Theory and Practice of Urban Sustainability Transitions, DOI 10.1007/978-3-319-56091-5_6.

Labib, S. M., & Harris, A., 2018. The potentials of Sentinel-2 and LandSat-8 data in green infrastructure extraction, using object based image analysis (OBIA) method. European Journal of Remote Sensing, 51(1), 231–240. https://doi.org/10.1080/22797254.2017.1419441

Li, X.; Zhou, W.Q.; Ouyang, Z.; Qian, Y.; Zhou, W.Q.; Li, W.; Han, L.; Yu, W.; Pickett, S.T.A.; Li, X.; et al.,2013. Relationship between land surface temperature and spatial pattern of greenspace: What are the effects of spatial resolution? Landsc. Urban Plan., 114, 1–8, doi:10.1016/j.landurbplan.2013.02.005.

Naeem, S., Cao, C., Waqar, M., Wei, C., & Acharya, B.,2018. Vegetation role in controlling the ecoenvironmental conditions for sustainable urban environments: A comparison of Beijing and Islamabad. Journal of Applied Remote Sensing, 12, 1. https://doi.org/10.1117/1.JRS.12.01601

McGarigal K., Marks BJ.,1995. Spatial pattern analysis program for quantifying landscape structure. Gen Tech Rep PNW-GTR-351 US Department of Agriculture, Forest Service, Pacific Northwest Research Station.

Park J., Kim J-H., Lee DK., Park CY., Jeong SG.,2017. The influence of small green space type and structure at the street level on urban heat island mitigation. Urban For Urban Green, 21:203–212.

Sobrino, J.A., Jimenez-Munoz, J.C., Soria, G., Romaguera, M., Guanter, L., Moreno, J., Plaza, A. Martinez, P., 2008. Land surface emissivity retrieval from different VNIR and TIR sensors. IEEETrans. Geosci. RemoteSens, 46, 316–327.

Suhet, 2015. Sentinel-2 User handbook. https://earth.esa.int/documents/247904/685211/Sentinel-2_User_Handbook.

Schwarz, N., Schlink, U., Franck, U., Großmann, K., 2012. Relationship of land surface and air temperatures and its implications for quantifying urban heat island indicators- an application for the city of Leipzig (Germany). Ecol. Indic. 18, 693–704.https://doi.org/10.1016/j.ecolind.2012.01.001.

Tran, H., Uchihama, D., Ochi, S., Yasuoka, Y., 2006. Assessment with satellite data of the urban heat island effects in Asian mega cities. Int. J. Appl. Earth Obs. Geoinf, 8, 34–48.

United States Geological Survey (USGS), 2019. Landsat 8 (L8) Data Users Handbook. https://www.usgs.gov/media/files/landsat-8-data-users-handbook

Xiangchen Meng, Jie Cheng, Shaohua Zhao, Sihan Liu, & Yunjun Yao 2018. Estimating Land Surface Temperature from Landsat-8 Data using the NOAA JPSS Enterprise Algorithm. Remote Sensing, 11(155), 1–18. https://doi.org/doi:10.3390/rs11020155

Yuan F, Bauer M., 2007. Comparison of impervious surface area and normalized difference vegetation index as indicators of surface urban heat island effects in Landsat imagery. Remote Sensing of Environment, 106, 375–386, http://dx.doi.org/10.1016/j.rse.2006.09.003.

Zha, Y., et al., 2003. Use of normalized difference built-up index in automatically mapping urban areas from TM imagery. International Journal of Remote Sensing, 24 (3), 583-594.

Zhou, W.; Wang, J.; Cadenasso, M.L., 2017. Effects of the spatial configuration of trees on urban heat mitigation: A comparative study. Remote Sens. Environ.2017, 195, 1-12, doi:10.1016/j.rse.2017.03.043.